Supporting Information

Materials Design of Sodium Chloride Solid Electrolytes

Na_3MCl_6 for All-Solid-State Sodium-Ion Batteries

Dongsu Park,[a,b] Kwangnam Kim,[c] Gin Hyung Chun,[a,b] Brandon C. Wood,[c] Joon Hyung Shim,[b,*] and Seungho Yu,[a,d,*]

[a]Energy Storage Research Center, Korea Institute of Science and Technology, 5, Hwarang-ro 14-gil, Seongbuk-gu, Seoul 02792, Republic of Korea

[b]School of Mechanical Engineering, Korea University, 145 Anam-ro, Seongbuk-gu, Seoul, 02841, South Korea

[c]Materials Science Division, Lawrence Livermore National Laboratory, Livermore, CA, 94550, USA

[d]Division of Energy & Environment Technology, KIST School, Korea University of Science and Technology, Seoul 02792, Republic of Korea

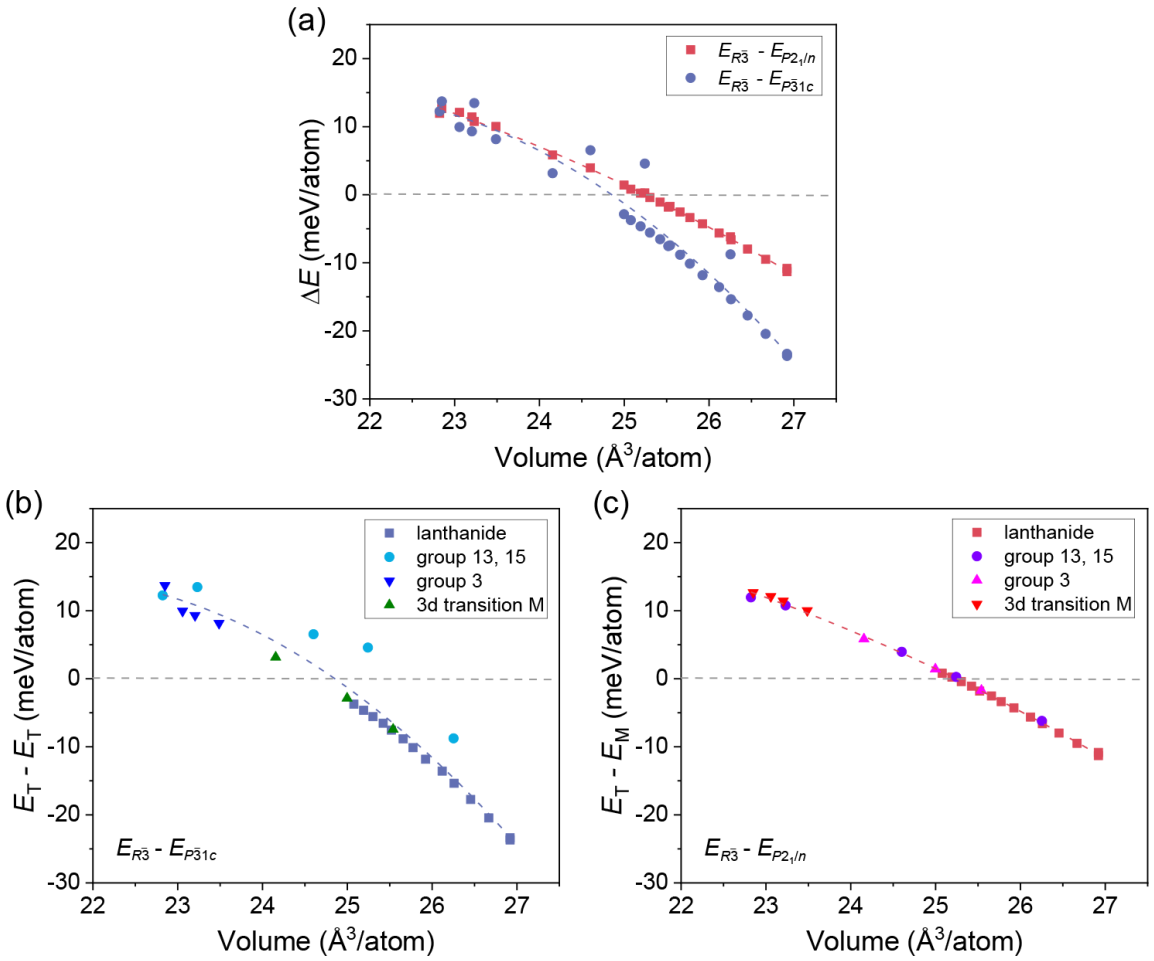

Fig. S1 (a-c) Energy difference between (b) trigonal $R\bar{3}$ and trigonal $P\bar{3}1c$, and (c) trigonal $R\bar{3}$ and monoclinic $P2_1/n$ structures of Na_3MCl_6 as a function of the volume of structures. The values in (b-c) were divided into four groups based on M: 3d transition metals, group 3 elements, group 13 and 15 elements, and lanthanides.

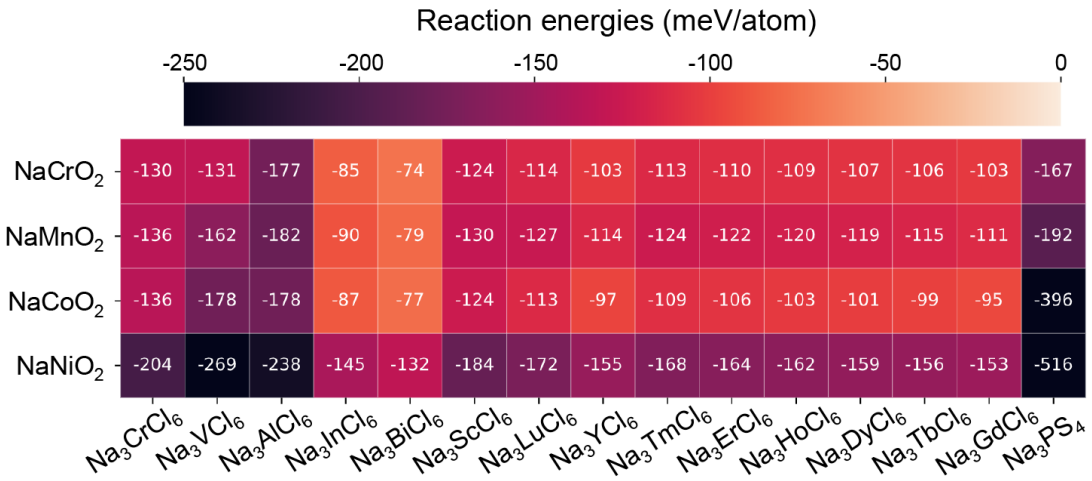

Fig. S2 Heat map of the reaction energy between Na_3MCl_6 and cathode materials.

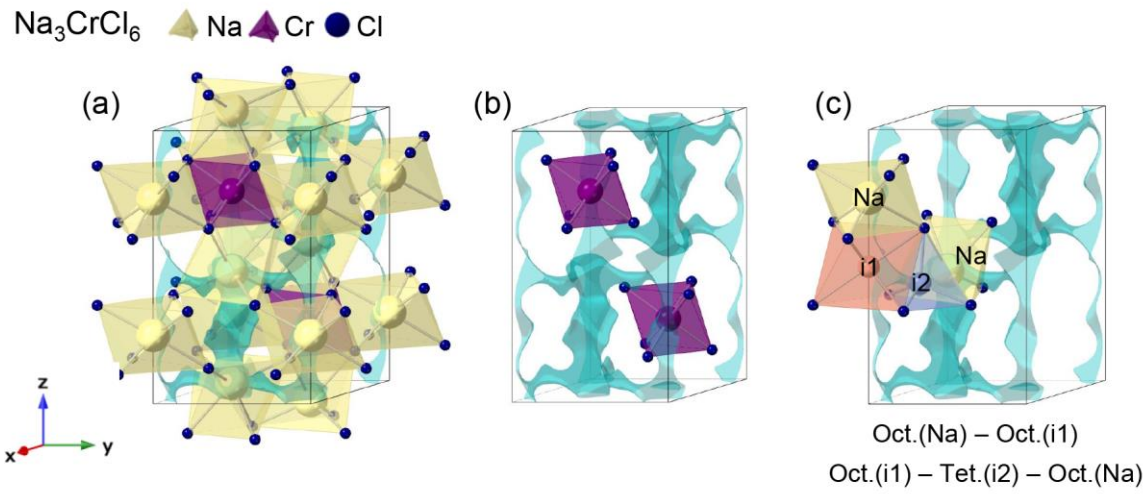

Fig. S3 Na-ion migration pathway in Na_3CrCl_6 (trigonal $P\bar{3}1c$) predicted by the BVSE method, representing (a-b) the isosurface of Na-ion migration path (light blue), and $NaCl_6$ and $CrCl_6$ octahedra (yellow and purple, respectively), (c) one-dimensional path between octahedral sites (Oct.–Oct.), and three-dimensional path between octahedral sites via tetrahedral interstitial sites (Oct.-Tet.-Oct.).

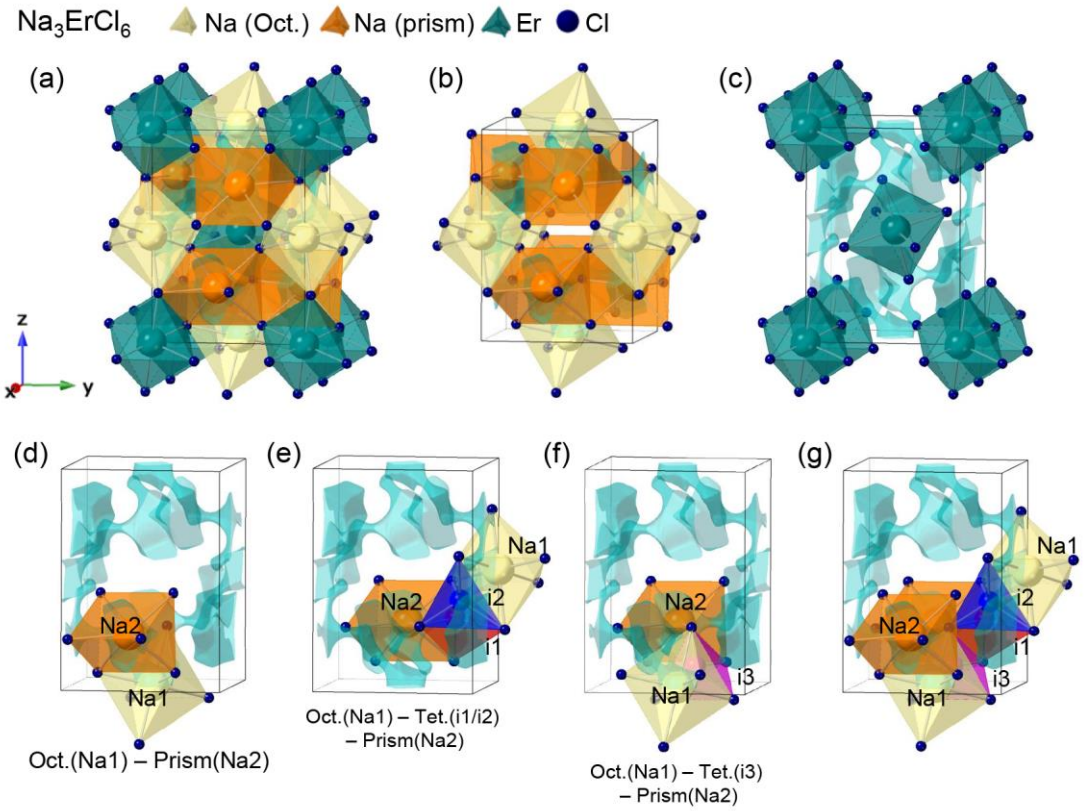

Fig. S4 Na-ion migration pathway in Na_3ErCl_6 (monoclinic $P2_1/n$) predicted by the BVSE method, representing (a-c) the isosurface of Na-ion migration path (light blue), and $NaCl_6$ octahedra, $NaCl_6$ prisms, and $ErCl_6$ octahedra (yellow, orange, and cyan-green, respectively), (d-g) migration paths between (d) octahedral and prism sites (Oct.–Prism), (e, f) octahedral and prism sites via tetrahedral interstitial sites (Oct.–Tet.–Prism).

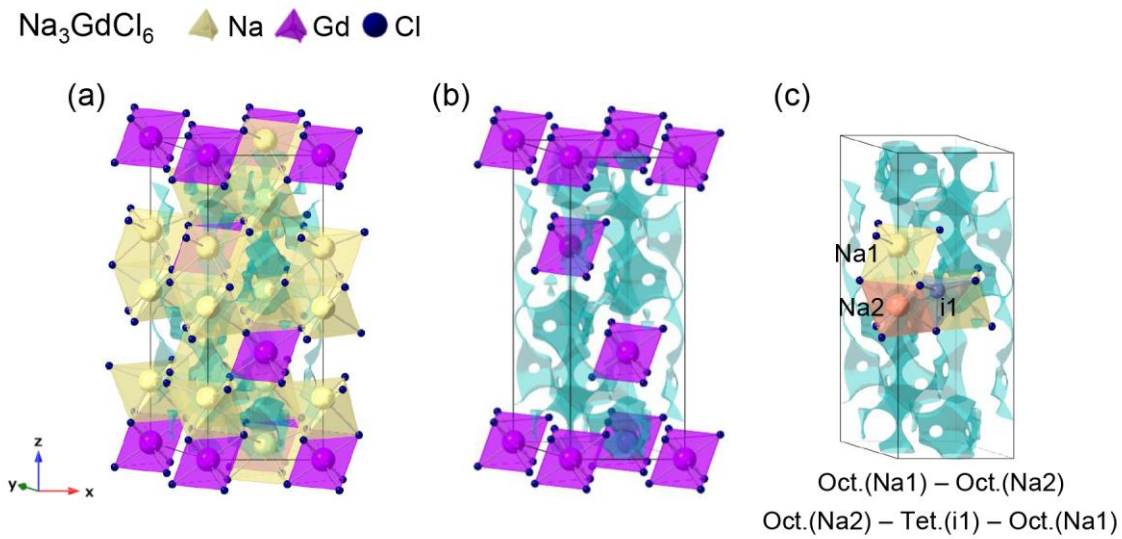

Fig. S5 Na-ion migration pathway in Na_3GdCl_6 (trigonal $R\bar{3}$) predicted by the BVSE method, representing (a-b) the isosurface of Na-ion migration path (light blue), and $NaCl_6$ and $GdCl_6$ octahedra (yellow and magenta, respectively), (c) one-dimensional path between octahedral sites (Oct.–Oct.), and three-dimensional path between octahedral sites via tetrahedral interstitial sites (Oct.–Tet.–Oct.).

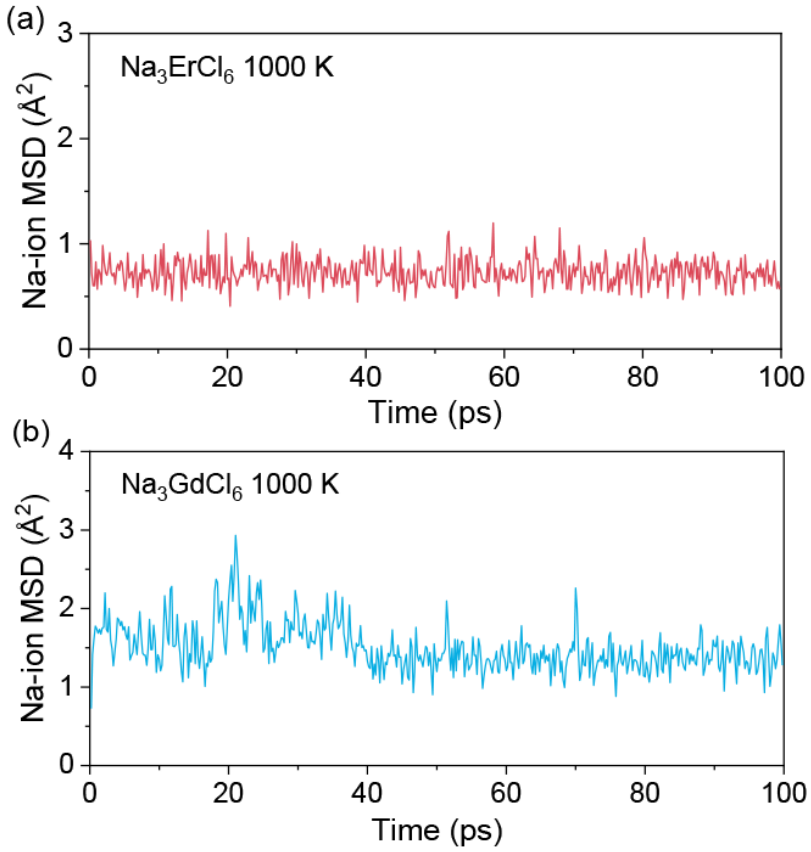

Fig. S6 Na-ion MSD over a 100-ps window for (a) Na_3ErCl_6 and (b) Na_3GdCl_6 at 1000 K.

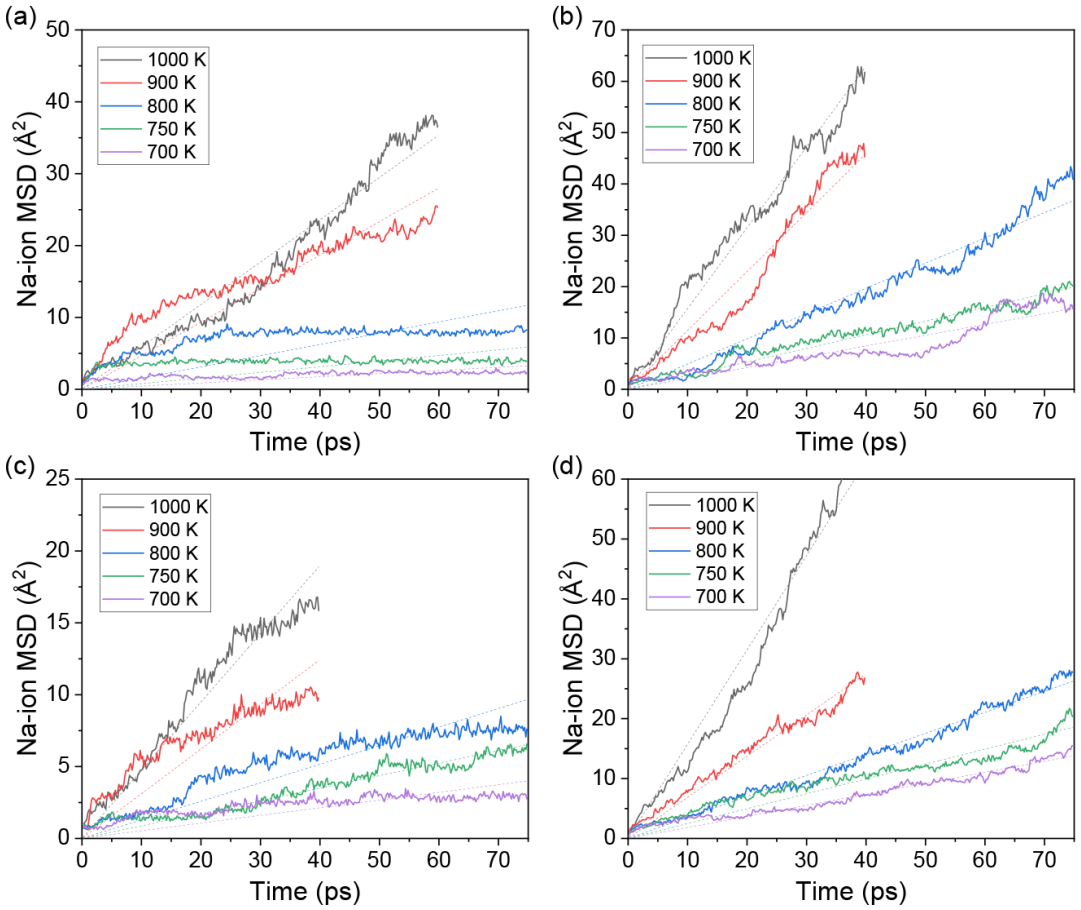

Fig. S7 Na-ion MSD at 750–1000 K for (a) Na_3CrCl_6, (b) $Na_{2.5}Cr_{0.5}Zr_{0.5}Cl_6$, (c) $Na_{2.5}Er_{0.5}Zr_{0.5}Cl_6$, and (d) $Na_{2.5}Gd_{0.5}Zr_{0.5}Cl_6$.

Table S1 Total energy differences among the crystal structures of the trigonal $P\bar{3}1c$ (S.G # 163), monoclinic $P2_1/n$ (S.G # 14), and trigonal $R\bar{3}$ (S.G # 148) for Na_3MCl_6.

	Na_3MCl_6	ΔE (meV/atom)		
		$R\bar{3}$ - $P21/n$ (T148 - M14)	$R\bar{3}$ - $P\bar{3}1c$ (T148-T163)	$P21/n$ - $P\bar{3}1c$ (M14-T163)
3d transition metal	Na_3CrCl_6	12.7	13.7	-1.0
	Na_3VCl_6	12.1	10.0	2.2
	Na_3FeCl_6	11.4	9.3	2.1
	Na_3TiCl_6	10.0	8.1	1.9
Group 3	Na_3ScCl_6	5.8	3.2	2.7
	Na_3LuCl_6	1.4	-2.9	4.3
	Na_3YCl_6	-1.7	-7.5	5.7
Group 13	Na_3AlCl_6	12.0	12.2	-0.3
	Na_3GaCl_6	10.8	13.5	-2.7
	Na_3InCl_6	4.0	6.5	-2.6
	Na_3TlCl_6	0.3	4.6	-4.3
Group 15	Na_3BiCl_6	-6.2	-8.8	2.6
Lanthanide	Na_3YbCl_6	0.8	-3.7	4.5
	Na_3TmCl_6	0.2	-4.6	4.9
	Na_3ErCl_6	-0.4	-5.6	5.2
	Na_3HoCl_6	-1.1	-6.5	5.5
	Na_3DyCl_6	-1.8	-7.5	5.7
	Na_3TbCl_6	-2.5	-8.8	6.3
	Na_3GdCl_6	-3.4	-10.1	6.8
	Na_3EuCl_6	-4.3	-11.8	7.5
	Na_3SmCl_6	-5.6	-13.6	7.9
	Na_3PmCl_6	-6.6	-15.4	8.8
	Na_3NdCl_6	-8.0	-17.7	9.8
	Na_3PrCl_6	-9.5	-20.5	11.0
	Na_3CeCl_6	-11.3	-23.7	12.4
	Na_3LaCl_6	-10.8	-23.4	12.5

Table S2. Volume of Na_3MCl_6 for the trigonal $P\bar{3}1c$, monoclinic $P2_1/n$, and trigonal $R\bar{3}$ structures.

	Na_3MCl_6	Volume (Å^3/atom)		
		Trigonal $P\bar{3}1c$ (S.G # 163)	Monoclinic $P2_1/n$ (S.G # 14)	Trigonal $R\bar{3}$ (S.G # 148)
3d transition metal	Na_3CrCl_6	23.76	21.87	22.92
	Na_3VCl_6	24.00	22.01	23.16
	Na_3FeCl_6	24.09	22.19	23.33
	Na_3TiCl_6	24.31	22.49	23.66
Group 3	Na_3ScCl_6	24.94	23.16	24.37
	Na_3LuCl_6	25.73	24.04	25.23
	Na_3YCl_6	26.22	24.63	25.76
Group 13	Na_3AlCl_6	23.76	21.83	22.88
	Na_3GaCl_6	24.11	22.25	23.33
	Na_3InCl_6	25.34	23.66	24.80
	Na_3TlCl_6	25.84	24.38	25.51
Group 15	Na_3BiCl_6	26.88	25.39	26.48
Lanthanide	Na_3YbCl_6	25.80	24.14	25.30
	Na_3TmCl_6	25.90	24.25	25.43
	Na_3ErCl_6	26.02	24.34	25.55
	Na_3HoCl_6	26.12	24.50	25.65
	Na_3DyCl_6	26.19	24.62	25.75
	Na_3TbCl_6	26.36	24.73	25.88
	Na_3GdCl_6	26.48	24.87	25.97
	Na_3EuCl_6	26.58	25.04	26.15
	Na_3SmCl_6	26.74	25.26	26.35
	Na_3PmCl_6	26.91	25.39	26.48
	Na_3NdCl_6	27.10	25.61	26.65
	Na_3PrCl_6	27.34	25.84	26.82
	Na_3CeCl_6	27.60	26.11	27.04
	Na_3LaCl_6	27.58	26.12	27.06

Table S3. Most stable phase of Na_3MCl_6 among the trigonal $P\bar{3}1c$, monoclinic $P2_1/n$, and trigonal $R\bar{3}$ phases from the experimental structures of Na_3MCl_6, and total energy differences (ΔE) between the stable phase of Na_3MCl_6 and monoclinic $C2/m$ or trigonal $P\bar{3}m1$ based on the experimental structures of Li_3MCl_6.

	Na_3MCl_6	Most stable phase	$E_{\text{tot, LMC phase}} - E_{\text{tot, stable phase}}$ (meV/atom)	
			ΔE against $C2/m$	ΔE against $P\bar{3}m1$
3d transition metal	Na_3CrCl_6	$P\bar{3}1c$	15.9	43.8
	Na_3VCl_6	$P2_1/n$	16.6	39.1
	Na_3FeCl_6	$P2_1/n$	16.0	38.8
	Na_3TiCl_6	$P2_1/n$	14.4	34.7
Group 3	Na_3ScCl_6	$P2_1/n$	12.0	28.6
	Na_3LuCl_6	$P2_1/n$	9.5	20.2
	Na_3YCl_6	$R\bar{3}$	9.6	16.6
Group 13	Na_3AlCl_6	$P\bar{3}1c$	16.3	42.6
	Na_3GaCl_6	$P\bar{3}1c$	14.4	42.3
	Na_3InCl_6	$P\bar{3}1c$	8.1	28.8
	Na_3TlCl_6	$P\bar{3}1c$	5.7	25.5
Group 15	Na_3BiCl_6	$R\bar{3}$	6.6	16.7
Lanthanide	Na_3YbCl_6	$P2_1/n$	9.1	19.1
	Na_3TmCl_6	$P2_1/n$	8.8	18.1
	Na_3ErCl_6	$R\bar{3}$	8.9	17.5
	Na_3HoCl_6	$R\bar{3}$	9.3	17.1
	Na_3DyCl_6	$R\bar{3}$	9.6	16.6
	Na_3TbCl_6	$R\bar{3}$	10.1	16.2
	Na_3GdCl_6	$R\bar{3}$	10.8	15.7
	Na_3EuCl_6	$R\bar{3}$	11.3	15.1
	Na_3SmCl_6	$R\bar{3}$	12.0	14.7
	Na_3PmCl_6	$R\bar{3}$	12.7	14.2
	Na_3NdCl_6	$R\bar{3}$	13.7	13.7
	Na_3PrCl_6	$R\bar{3}$	14.8	13.2
	Na_3CeCl_6	$R\bar{3}$	16.2	12.6
	Na_3LaCl_6	$R\bar{3}$	15.8	12.3

Table S4. Phase stability (energy above the convex hull, E_{hull}) of Na_3MCl_6 with the crystal structures of $P\bar{3}1c$, $P2_1/n$, $R\bar{3}$, $C2/m$, and $P\bar{3}m1$, and corresponding decomposition phases.

M	Na_3MCl_6	E_{hull} (meV/atom)						Stability	Decomp. phases
		Trigonal $P\bar{3}1c$ (S.G # 163)	Monoclinic $P2_1/n$ (S.G # 14)	Trigonal $R\bar{3}$ (S.G # 148)	Monoclinic $C2/m$ (S.G # 12)	Trigonal $P\bar{3}m1$ (S.G # 164)	Most stable phase		
3d transition metal	Na_3CrCl_6	14	16	28	30	58	$P\bar{3}1c$	Meta-Stable	$CrCl_3$, NaCl
	Na_3VCl_6	25	22	35	39	62	$P2_1/n$	Meta-Stable	VCl_3, NaCl
	Na_3FeCl_6	29	27	39	43	66	$P2_1/n$	Unstable	$NaFeCl_4$, NaCl
	Na_3TiCl_6	28	26	36	41	61	$P2_1/n$	Unstable	$TiCl_3$, NaCl
Group 3	Na_3ScCl_6	-2	-5	1	8	24	$P2_1/n$	Stable	$NaScCl_4$, NaCl
	Na_3LuCl_6	-3	-7	-5	3	13	$P2_1/n$	Stable	$NaLuCl_4$, NaCl
	Na_3YCl_6	-3	-9	-11	-1	6	$R\bar{3}$	Stable	YCl_3, NaCl
Group 13	Na_3AlCl_6	22	22	34	38	64	$P\bar{3}1c$	Meta-Stable	$NaAlCl_4$, NaCl
	Na_3GaCl_6	41	44	55	56	84	$P\bar{3}1c$	Unstable	$NaGaCl_4$, NaCl
	Na_3InCl_6	-4	-2	2	4	25	$P\bar{3}1c$	Stable	$InCl_3$, NaCl
	Na_3TlCl_6	-2	3	3	4	24	$P\bar{3}1c$	Stable	$TlCl_3$, NaCl
Group 15	Na_3BiCl_6	-1	-4	-10	-3	7	$R\bar{3}$	Stable	$BiCl_3$, NaCl
Lanthanide	Na_3YbCl_6	-6	-10	-9	-1	9	$P2_1/n$	Stable	$YbCl_3$, NaCl
	Na_3TmCl_6	-1	-6	-6	3	12	$P2_1/n$	Stable	$NaTmCl_4$, NaCl
	Na_3ErCl_6	3	-2	-3	6	15	$R\bar{3}$	Stable	$ErCl_3$, NaCl
	Na_3HoCl_6	8	3	1	11	18	$R\bar{3}$	Meta-Stable	$HoCl_3$, NaCl
	Na_3DyCl_6	13	7	6	15	22	$R\bar{3}$	Meta-Stable	$DyCl_3$, NaCl
	Na_3TbCl_6	15	9	6	17	23	$R\bar{3}$	Meta-Stable	$NaTbCl_4$, NaCl
	Na_3GdCl_6	25	19	15	26	31	$R\bar{3}$	Meta-Stable	$GdCl_3$, NaCl
	Na_3EuCl_6	34	27	22	34	38	$R\bar{3}$	Meta-Stable	$EuCl_3$, NaCl
	Na_3SmCl_6	43	35	30	42	45	$R\bar{3}$	Unstable	$SmCl_3$, NaCl
	Na_3PmCl_6	52	43	36	49	50	$R\bar{3}$	Unstable	$PmCl_3$, NaCl
	Na_3NdCl_6	61	51	43	57	57	$R\bar{3}$	Unstable	$NdCl_3$, NaCl
	Na_3PrCl_6	70	60	50	65	63	$R\bar{3}$	Unstable	$PrCl_3$, NaCl
	Na_3CeCl_6	80	68	57	73	69	$R\bar{3}$	Unstable	$CeCl_3$, NaCl
	Na_3LaCl_6	76	64	53	69	65	$R\bar{3}$	Unstable	$LaCl_3$, NaCl

Table S5. Crystal structure of MCl_3 including space group, ICSD IDs, and MP-IDs.

M	M	M_{Radii} (pm)	MCl_3	Space group	Crystal system	ICSD IDs	MP-IDs	Structure
3d transition metal	Cr	61.5	$CrCl_3$	R-3	trigonal	22081	mp-567504	
	V	64	VCl_3	R-3	trigonal	38237	mp-28117	
	Fe	64.5	$FeCl_3$	R-3	trigonal			substitution from $ScCl_3$
	Ti	67	$TiCl_3$	P6_3/mcm	hexagonal	26069	mp-571143	
Group 3	Sc	74.5	$ScCl_3$	R-3	trigonal	74517	mp-23309	
	Lu	86.1	$LuCl_3$	C2/m	monoclinic			substitution from YCl_3
	Y	90	YCl_3	C2/m	monoclinic	15684	mp-27455	
Group 13	Al	53.5	$AlCl_3$	C2/m	monoclinic	39566	mp-25469	
	Ga	62	$GaCl_3$	C2/m	monoclinic	413455	mp-30952	
	In	80	$InCl_3$	C2/m	monoclinic			substitution from YCl_3
	Tl	88.5	$TlCl_3$	C2/m	monoclinic			substitution from YCl_3
Group 15	Bi	103	$BiCl_3$	Pnma	orthorhombic	41179	mp-22908	
Lanthanide	Yb	86.8	$YbCl_3$	C2/m	monoclinic			substitution from YCl_3
	Tm	88	$TmCl_3$	R-3c	trigonal	35398	mp-28044	
	Er	89	$ErCl_3$	Cmcm	orthorhombic			substitution from $DyCl_3$
	Ho	90.1	$HoCl_3$	Cmcm	orthorhombic			substitution from $DyCl_3$
	Dy	91.2	$DyCl_3$	Cmcm	orthorhombic	40064	mp-28448	
	Tb	92.3	$TbCl_3$	P4_2/mnm	tetragonal	63543	mp-570232	
	Gd	93.5	$GdCl_3$	P6_3/m	hexagonal	15387	mp-23265	
	Eu	94.7	$EuCl_3$	P6_3/m	hexagonal	23148	mp-569895	
	Sm	95.8	$SmCl_3$	P6_3/m	hexagonal			substitution from $NdCl_3$
	Pm	97	$PmCl_3$	P6_3/m	hexagonal			substitution from $NdCl_3$
	Nd	98.3	$NdCl_3$	P6_3/m	hexagonal	23147	mp-23183	
	Pr	99	$PrCl_3$	P6_3/m	hexagonal	65079	mp-23211	
	Ce	101	$CeCl_3$	P6_3/m	hexagonal	31575	mp-582011	
	La	103.2	$LaCl_3$	P6_3/m	hexagonal	31574	mp-22896	

Table S6. Energy difference of MCl_3 compared to the compounds with the lowest energy among 8 phases. For example, $LuCl_3$ exhibits the lowest total energy for the *C*2/*m* structure (YCl_3 structure) among 8 phases, and the values show the total energy difference compared to the energy of *C*2/*m* structure.

MCl_3	$E_{tot} - E_{tot,\ lowest\ E}$ (meV/atom)								Most stale phase
	R-3 ($ScCl_3$)	R-3c ($TmCl_3$)	P4_2/mnm ($TbCl_3$)	Cmcm ($DyCl_3$)	Pnma ($BiCl_3$)	C2/m (YCl_3)	P6_3/mcm ($TiCl_3$)	P6_3/m ($NdCl_3$)	
$LuCl_3$	1	19	15	15	51	0	82	45	C2/m
$InCl_3$	1	61	43	112	70	0	68	190	C2/m
$TlCl_3$	2	41	29	124	73	0	61	92	C2/m
$FeCl_3$	0	76	59	94	42	1	40	179	R-3
$YbCl_3$	1	17	14	3	40	0	82	29	C2/m
$ErCl_3$	20	29	28	0	37	18	100	17	Cmcm
$HoCl_3$	31	38	39	0	36	30	111	12	Cmcm
$SmCl_3$	107	97	105	14	40	104	181	0	P6_3/m
$PmCl_3$	124	110	120	19	43	120	196	0	P6_3/m

Table S7. Phase equilibria and decomposition energy, E_D, for the reduction reaction of Na_3MCl_6 with Na metal.

Na_3MCl_6	Phase equilibria with Na metal	E_D (eV/atom)
Na_3CrCl_6	Cr, NaCl	-0.633
Na_3VCl_6	V, NaCl	-0.593
Na_3AlCl_6	Al, NaCl	-0.470
Na_3InCl_6	Na_2In, NaCl	-0.658
Na_3BiCl_6	Na_3Bi, NaCl	-0.820
Na_3ScCl_6	Sc, NaCl	-0.219
Na_3LuCl_6	Lu, NaCl	-0.154
Na_3YCl_6	Y, NaCl	-0.155
Na_3TmCl_6	Tm, NaCl	-0.153
Na_3ErCl_6	Er, NaCl	-0.153
Na_3HoCl_6	Ho, NaCl	-0.153
Na_3DyCl_6	Dy, NaCl	-0.154
Na_3TbCl_6	Tb, NaCl	-0.154
Na_3GdCl_6	Gd, NaCl	-0.169

Table S8. Reduction and oxidation potentials of Na_3MCl_6 with corresponding phase equilibria.

Na_3MCl_6	Reduction potential (V)	Phase equilibria at the reduction potential	Oxidation potential (V)	Phase equilibria at the oxidation potential
Na_3CrCl_6	2.09	Cr, NaCl	3.75	$NaCl_3$, $CrCl_3$
Na_3VCl_6	2.11	VCl_2, NaCl	2.82	VCl_4, NaCl
Na_3AlCl_6	1.49	Al, NaCl	3.75	$NaCl_3$, $NaAlCl_4$
Na_3InCl_6	2.14	$InCl_2$, NaCl	4.07	$NaCl_3$, $InCl_3$
Na_3BiCl_6	2.24	Bi, NaCl	3.93	$NaCl_3$, $BiCl_3$
Na_3ScCl_6	0.75	Sc_5Cl_8, NaCl	3.82	$NaCl_3$, $ScCl_3$
Na_3LuCl_6	0.51	Lu, NaCl	3.85	$NaCl_3$, $NaLuCl_4$
Na_3YCl_6	0.52	Y, NaCl	3.81	$NaCl_3$, YCl_3
Na_3TmCl_6	0.51	Tm, NaCl	3.86	$NaCl_3$, $NaTmCl_4$
Na_3ErCl_6	0.51	Er, NaCl	3.84	$NaCl_3$, $NaErCl_4$
Na_3HoCl_6	0.51	Ho, NaCl	3.91	$NaCl_3$, $NaHoCl_4$
Na_3DyCl_6	0.51	Dy, NaCl	3.88	$NaCl_3$, $NaDyCl_4$
Na_3TbCl_6	0.51	Tb, NaCl	3.86	$NaTbCl_4$, $NaCl_3$
Na_3GdCl_6	0.59	Gd_2Cl_3, NaCl	3.77	$NaGdCl_4$, $NaCl_3$

Table S9. Volume, energy above the hull, E_{hull}, and decomposition phases of Zr-substituted $Na_{3-x}M_{1-x}Zr_xCl_6$ (M= Cr, Er, and Gd; x= 0, 0.25, 0.5, 0.75, and 1)

$Na_{3-x}M_{1-x}Zr_xCl_6$	x	Composition	Volume ($Å^3$/atom)	E_{hull} (meV/atom)	Decomposition phases
$Na_{3-x}Cr_{1-x}Zr_xCl_6$	0	Na_3CrCl_6	23.76	14.5	NaCl, $CrCl_3$
	0.25	$Na_{2.75}Cr_{0.75}Zr_{0.25}Cl_6$	24.47	12.4	NaCl, $CrCl_3$, $ZrCl_4$
	0.50	$Na_{2.5}Cr_{0.5}Zr_{0.5}Cl_6$	25.29	7.3	
	0.75	$Na_{2.25}Cr_{0.25}Zr_{0.75}Cl_6$	26.26	10.3	
$Na_{3-x}Er_{1-x}Zr_xCl_6$	0	Na_3ErCl_6	25.55	-2.7	NaCl, $ErCl_3$
	0.25	$Na_{2.75}Er_{0.75}Zr_{0.25}Cl_6$	24.59	-1.4	NaCl, $ErCl_3$, $ZrCl_4$
	0.50	$Na_{2.5}Er_{0.5}Zr_{0.5}Cl_6$	24.84	-1.4	
	0.75	$Na_{2.25}Er_{0.25}Zr_{0.75}Cl_6$	25.21	-6.3	
$Na_{3-x}Gd_{1-x}Zr_xCl_6$	0	Na_3GdCl_6	25.97	15.2	NaCl, $GdCl_3$
	0.25	$Na_{2.75}Gd_{0.75}Zr_{0.25}Cl_6$	26.20	15.4	NaCl, $GdCl_3$, $ZrCl_4$
	0.50	$Na_{2.5}Gd_{0.5}Zr_{0.5}Cl_6$	26.30	14.3	
	0.75	$Na_{2.25}Gd_{0.25}Zr_{0.75}Cl_6$	26.37	4.8	
Na_2ZrCl_6		Na_2ZrCl_6	25.79	-21.4	NaCl, $ZrCl_4$

Table S10. Reduction and oxidation potentials of $Na_{2.5}Cr_{0.5}Zr_{0.5}Cl_6$, $Na_{2.5}Er_{0.5}Zr_{0.5}Cl_6$, $Na_{2.5}Gd_{0.5}Zr_{0.5}Cl_6$, and Na_2ZrCl_6 with corresponding phase equilibria.

Composition	Reduction potential (V)	Phase equilibria at the reduction potential	Oxidation potential (V)	Phase equilibria at the oxidation potential
$Na_{2.5}Cr_{0.5}Zr_{0.5}Cl_6$	2.09	$ZrCl_4$, NaCl, Cr	3.75	$NaCl_3$, $ZrCl_4$, $CrCl_3$
$Na_{2.5}Er_{0.5}Zr_{0.5}Cl_6$	1.70	$ZrCl_3$, Na_3ErCl_6, NaCl	3.75	Na_3ErCl_6, $NaCl_3$, $ZrCl_4$
$Na_{2.5}Gd_{0.5}Zr_{0.5}Cl_6$	1.70	$ZrCl_3$, $NaGdCl_4$, NaCl	3.75	$NaGdCl_4$, $NaCl_3$, $ZrCl_4$
Na_2ZrCl_6	1.51	$ZrCl_2$, NaCl	3.92	$NaCl_3$, $ZrCl_4$

Table S11. Volume and energy above the hull, E_{hull} of $Na_{3-x}A_{1-x}B_xCl_6$ (A= Cr, Er, and Gd; B= Ti and Hf; x= 0, 0.25, 0.5, 0.75, and 1)

	x	Composition	Volume (Å^3/atom)	E_{hull} (meV/atom)	Decomposition phases
$Na_{3-x}Cr_{1-x}Ti_xCl_6$	0	Na_3CrCl_6	23.76	14.5	NaCl, $CrCl_3$
	0.25	$Na_{2.75}Cr_{0.75}Ti_{0.25}Cl_6$	24.19	17.6	NaCl, $CrCl_3$, $TiCl_4$
	0.50	$Na_{2.5}Cr_{0.5}Ti_{0.5}Cl_6$	24.60	17.7	
	0.75	$Na_{2.25}Cr_{0.25}Ti_{0.75}Cl_6$	25.30	27.9	
$Na_{3-x}Er_{1-x}Ti_xCl_6$	0	Na_3ErCl_6	25.55	-2.7	NaCl, $ErCl_3$
	0.25	$Na_{2.75}Er_{0.75}Ti_{0.25}Cl_6$	24.26	4.6	NaCl, $ErCl_3$, $TiCl_4$
	0.50	$Na_{2.5}Er_{0.5}Ti_{0.5}Cl_6$	24.21	11.1	
	0.75	$Na_{2.25}Er_{0.25}Ti_{0.75}Cl_6$	24.14	11.5	
$Na_{3-x}Gd_{1-x}Ti_xCl_6$	0	Na_3GdCl_6	25.97	15.2	NaCl, $GdCl_3$
	0.25	$Na_{2.75}Gd_{0.75}Ti_{0.25}Cl_6$	25.91	23.9	NaCl, $GdCl_3$, $TiCl_4$
	0.50	$Na_{2.5}Gd_{0.5}Ti_{0.5}Cl_6$	25.67	29.9	
	0.75	$Na_{2.25}Gd_{0.25}Ti_{0.75}Cl_6$	25.33	25.6	
$Na_{3-x}Cr_{1-x}Hf_xCl_6$	0	Na_3CrCl_6	23.76	14.5	NaCl, $CrCl_3$
	0.25	$Na_{2.75}Cr_{0.75}Hf_{0.25}Cl_6$	24.37	11.2	NaCl, $CrCl_3$, $HfCl_4$
	0.50	$Na_{2.5}Cr_{0.5}Hf_{0.5}Cl_6$	25.01	4.5	
	0.75	$Na_{2.25}Cr_{0.25}Hf_{0.75}Cl_6$	26.08	5.7	
$Na_{3-x}Er_{1-x}Hf_xCl_6$	0	Na_3ErCl_6	25.55	-2.7	NaCl, $ErCl_3$
	0.25	$Na_{2.75}Er_{0.75}Hf_{0.25}Cl_6$	24.73	-2.6	NaCl, $ErCl_3$, $HfCl_4$
	0.50	$Na_{2.5}Er_{0.5}Hf_{0.5}Cl_6$	24.79	-3.7	
	0.75	$Na_{2.25}Er_{0.25}Hf_{0.75}Cl_6$	25.10	-10.0	
$Na_{3-x}Gd_{1-x}Hf_xCl_6$	0	Na_3GdCl_6	25.97	15.2	NaCl, $GdCl_3$
	0.25	$Na_{2.75}Gd_{0.75}Hf_{0.25}Cl_6$	26.17	14.4	NaCl, $GdCl_3$, $HfCl_4$
	0.50	$Na_{2.5}Gd_{0.5}Hf_{0.5}Cl_6$	26.20	12.4	
	0.75	$Na_{2.25}Gd_{0.25}Hf_{0.75}Cl_6$	26.23	1.5	